ELSEVIER

Journal of Nuclear Materials 307–311 (2002) 1578–1583

journal of nuclear materials

www.elsevier.com/locate/jnucmat

Re-weldability of neutron-irradiated stainless steels studied by multi-pass TIG welding

K. Nakata [a,*,1], M. Oishi [a], M. Koshiishi [b,1], T. Hashimoto [b], H. Anzai [b], Y. Saito [c], W. Kono [c]

[a] *Tokyo Engineering Center, Japan Power Engineering and Inspection Corporation (JAPEIC), Mihama, Urayasu-shi, Chiba 279-0011, Japan*

[b] *Hitachi Ltd., 3-1-1, Saiwai-cho, Hitachi, Ibaraki 317-0073, Japan*

[c] *Toshiba Corporation, 8 Shinsugita-cho, Isogo-ku, Yokohama, Kanagawa 235-8523, Japan*

Abstract

Weldability of neutron-irradiated stainless steel (SS) has been studied by multi-pass bead-on-plate and build-up tungsten inert gas (TIG) welding, simulating the repair-welding of reactor components. Specimens were submerged arc welding (SAW) joint of Type 304 SS containing 0.5 appm helium (1.8 appm in the SAW weld metal). Sound welding could be obtained by one- to three-pass welding on the plates at weld heat inputs less than 1 MJ/m in the irradiated 304 SS base metal. In the case of the build-up welding of a groove, no visible defects appeared in the specimen at a heat input as low as 0.4 MJ/m. However, build-up welding at a high heat input of 1 MJ/m was prone to weld cracking, owing to the formation of helium bubbles on grain boundaries of the base metal or dendrite boundaries of pre-existing SAW weld metal, in the area within 0.6 mm from the fusion line.

1. Introduction

The life extension of fusion and fission reactors needs the repairs of irradiation-degraded components. Welding could represent one of the principle methods for repairing and replacing such components. Welding techniques have been extensively studied in the last decades, and studies pointed out that welding was not always successful in neutron-irradiated stainless steels (SSs) [1].

Weld cracks of irradiated SSs generally occurred in the weld heat affected zone (HAZ) [2]. These cracks had an intergranular nature, and this feature was attributed to the nucleation, coalescence and growth of helium bubbles along grain boundaries. These phenomena were due to the thermal cycle and thermal stress related to welding process [3,4]. Helium bubbles on grain boundaries and the presence of dimples on fracture surfaces have been shown by scanning and transmission electron microscopy [1,3,5,6]. The degree of cracking decreased with helium concentration, but the cracking susceptibility was not eliminated also in SSs containing less than 1 appm helium [1,7]. Weld heat input was identified as another important parameter for welding of irradiated materials [7]. Low-heat-input weld techniques reduce the size of the HAZ and the width of high stress regions in the substrate material, resulting in the suppression of weld cracking [8,9].

In this work, the weldability of neutron-irradiated stainless steels is studied by multi-pass tungsten inert gas (TIG) welding. Consideration is given to build-up repair-welding of reactor components.

This work was performed as a part of the project 'Repair-Welding Technology of Irradiated Materials' entrusted to JAPEIC by the METI.

* Corresponding author. Tel.: +81-29 267 9003; fax: +81-29 266 2589.

E-mail address: k_nakata@nfd.co.jp (K. Nakata).

[1] Present address: Nuclear Fuel Development, 2163, Narita-cho, Oarai-machi, Higashi-Ibaraki, Ibaraki 311-1313, Japan.

0022-3115/02/$ - see front matter
PII: S0022-3115(02)00966-2

2. Experimental procedure

Specimens were made from a Type 304 SS plate (Fe–0.06 wt%C–0.71 wt%Si–0.02 wt%P–0.001 wt%S–8.44 wt%Ni–18.23 wt%Cr–2 wtppmB) with a SAW joint. Chemical composition of the filler wire for SAW was Type 308 (Fe–0.06 wt%C–0.77 wt%Si–0.02 wt%P–0.004 wt%S–9.68 wt%Ni–20.76 wt%Cr–7 wtppmB). Two kinds of specimens were prepared: one was a Type 304 SS plate of $60 \times 100 \times 10$ mm^3, and the other was a 20 mm thick plate with a groove of 10 mm depth, which had been cut in the HAZ of the SAW weld [10].

The specimens were irradiated up to 6.3×10^{23} n/m^2 (>1 MeV) and 7.0×10^{23} n/m^2 (<0.414 eV) at an irradiation temperature below 473 K by the ATR, INEEL [10]. Helium concentrations after the irradiation was measured by a mass spectrograph: typical values were about 0.5 and 1.8 appm in the Type 304 base metal and the SAW weld metal, respectively. That difference in helium concentrations was mainly caused by a difference on initial boron concentrations of the different zones of the joint.

Welding tests were performed in a hot laboratory by a TIG welding technique, using a Type 308L SS filler wire of 0.9 mm in diameter. The one-pass and three-pass bead-on-plate welding tests were made in the 10 mm thick specimens at heat inputs of 0.2, 0.4 and 1 MJ/m. Build-up welding of a groove in the 20 mm thick specimens was performed at 0.4 and 1 MJ/m. Beads were deposited at an interval of about 300 s. The welding parameters were pre-selected using unirradiated specimens. Particular care was given to constraint of the specimen during welding in order to avoid distortion.

3. Results

TIG weldings of irradiated specimens were carried out using heat inputs ranging from 0.2 to 1 MJ/m. In the build-up welding of a groove, the total number of passes was 16 and 50 for the 1 and 0.4 MJ/m welding process, respectively: one layer was mostly made by one-pass at 1 MJ/m, and by two passes at 0.4 MJ/m. The penetrant test (PT) was performed after welding to inspect surface cracks. No cracks appeared in the specimens, except for the 1 MJ/m build-up welded specimen. Fig. 1 shows the appearance of a PT examination in the 1 MJ/m build-up welded specimen. Slight indications of PT are observed along the fusion line on the side of the SAW weld metal, while none appears in 304 SS base metal.

Cross-sectional observations were carried out by optical microscopy. Unetched and etched structures of each specimen were compared in order to confirm the occurrence of cracks or traces of helium bubbles. The results are summarized in Table 1. The specimens did not present cracks and weld defects along grain boundaries of HAZ and weld metal, except in the case of the 1 MJ/m build-up welded specimen.

The location of weld defects in a cross-section of the 1 MJ/m build-up welded specimen is shown in Fig. 2. Typical cross-sectional micrographs are shown in Fig. 3

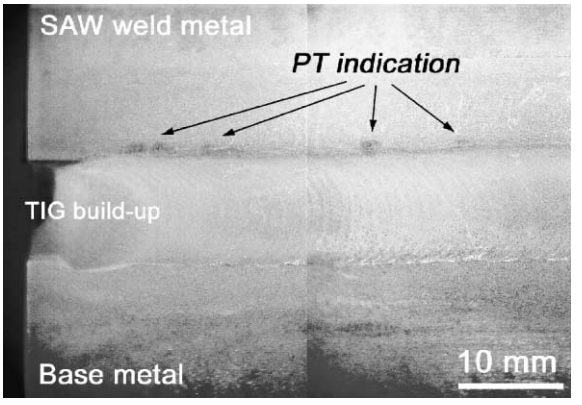

Fig. 1. PT result after the 1 MJ/m TIG build-up welding in an irradiated specimen. Helium concentrations are about 0.5 and 1.8 appm helium in the base metal and pre-existing SAW weld metal, respectively.

Table 1
Results of cross-sectional observation in weld HAZ of the specimens

Weld heat input (MJ/m)	Bead-on-plate welding		Build-up welding	
	One-pass	Three-pass	Base metal	SAW weld metal
0.2	No cracks No weld defects	No cracks No weld defects	–	–
0.4	No cracks No weld defects	No cracks No weld defects	No cracks No weld defects	No cracks No weld defects
1	No cracks No weld defects	No cracks No weld defects	No cracks Defects on grain boundaries	Cracks Defects on dendrite boundaries

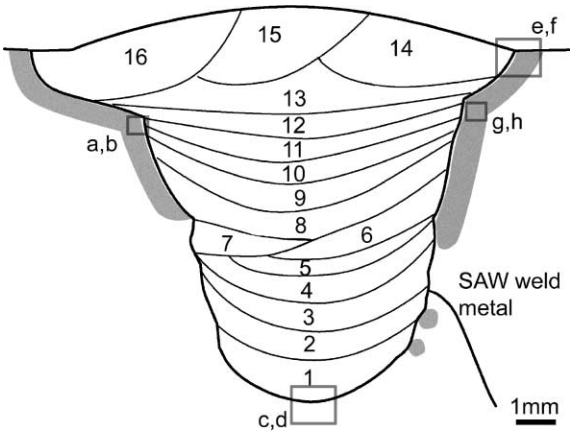

Fig. 2. Build-up sequence and regions of welding defects (shadow) in a cross-section of the 1 MJ/m build-up welded specimen, as obtained by cross-sectional observation using optical microscopy. Squares indicate the observation areas for micrographs shown in Fig. 3.

for analyzed areas indicated in Fig. 2. Most defects produced by the welding process are within about 0.6 mm from the fusion line and about 5 mm in depth from the surface. The highest density of defects is found around 0.2 mm from the fusion line. In the base metal, dot defects of 1–4 μm in diameter are aligned on grain boundaries and some defects are interconnected, which give the appearance of small intergranular cracks (Fig. 3(a) and (b)). These aligned defects show a tendency to become parallel to the fusion line. However, no visible defects are found in the lower part of the groove (Fig. 3(c) and (d)). A crack, about 0.2 mm long, appears under the surface on the side of the SAW weld metal (Fig. 3(e)). The micrograph of etched specimen clearly reveals the interdendritic cracking nature of that flaw (Fig. 3(f)). A lot of interconnected dot defects are observed on dendrite boundaries (Fig. 3(g) and (h)). Although the related micrographs are not shown, neither visible cracks nor aligned defects on grain or dendrite boundaries were found in the 0.4 MJ/m build-up welded specimen as well as in any bead-on-plate welded specimens.

4. Discussion

When the irradiated SS containing 0.5–1.8 appm helium was build-up welded by TIG welding at 1 MJ/m, dot defects were preferentially observed on grain boundaries and dendrite boundaries (Fig. 3). These are not observed in the unirradiated specimen, then they seem to be helium bubbles formed during the welding process. Moreover, they were only found in the area within about 0.6 mm from the fusion line. From a heat conduction analysis, the temperature of this area increases up to about 1400 K: helium atoms can more easily migrate only at high temperature because of their large migration energy [11]. This behavior reinforces the speculation that the defects are related to helium bubbles. The observations indicate that the dendrite boundaries also act as preferential nucleation sites of helium bubbles, as grain boundaries do.

Density of the helium bubble can be theoretically predicted by rate equations considering aggregation of helium–vacancy complexes and coalescence of small bubbles on the boundary [12,13]. The growth of helium bubbles is mainly controlled by the tensile stress generated during the cooling phase of welding, and the growth rate is given by the Hull–Rimmer equation [3,14]. Using these analytical methods, helium bubble diameter was estimated for the conditions of our experimental study. The thermal profile was obtained by a heat conduction calculation taking into account a moving heat source. From the results of thermal elastic–plastic analysis, the strain during the cooling phase is generally larger than 0.2% near the fusion line [15] and work hardening is negligible at elevated temperatures. Therefore, the tensile stress in that area was considered equivalent to the proof stress [10]. Considering a one-pass bead-on-plate welding, in the material containing 0.5 appm helium, and 0.2 mm far from the fusion line, the calculated helium bubble diameters are 180, 260 and 500 nm for heat inputs of 0.2, 0.4 and 1 MJ/m, respectively. It is evident that the higher the heat flux, the larger the bubbles; nevertheless, the bubble density seems insensitive to heat input, remaining at almost the same value, $8 \times 10^{11}/m^2$. It is thought that the cooling rate is inversely correlated to the heat input, then helium bubbles remain at high temperatures for a time sufficiently long to grow in a high heat input welding process,. Since helium bubbles grow during every weld pass, after the three-pass welding process the bubble diameter is approximately 1.7 times larger than that of the one-pass welding at each heat input. The bubble density is not changed by repeated thermal cycles, because bubble nucleation and coalescence occur only during the first cycle.

The changes in helium bubble diameter at the neck and bottom points of the groove (0.2 mm from the fusion line) are shown in Fig. 4 for the build-up welding at 1 MJ/m. At the bottom point, the fusion metal is deposited by every welding pass, the heat source moves away and the maximum temperature quickly decreases at each cycle. Therefore, hardly any helium bubbles can grow after the fourth pass and the bubble size remains small. On the other hand, the groove width at the neck point is broad compared with that at the bottom, and several fusion lines are close to the neck point, as shown in Fig. 2. At least three severe thermal cycles are

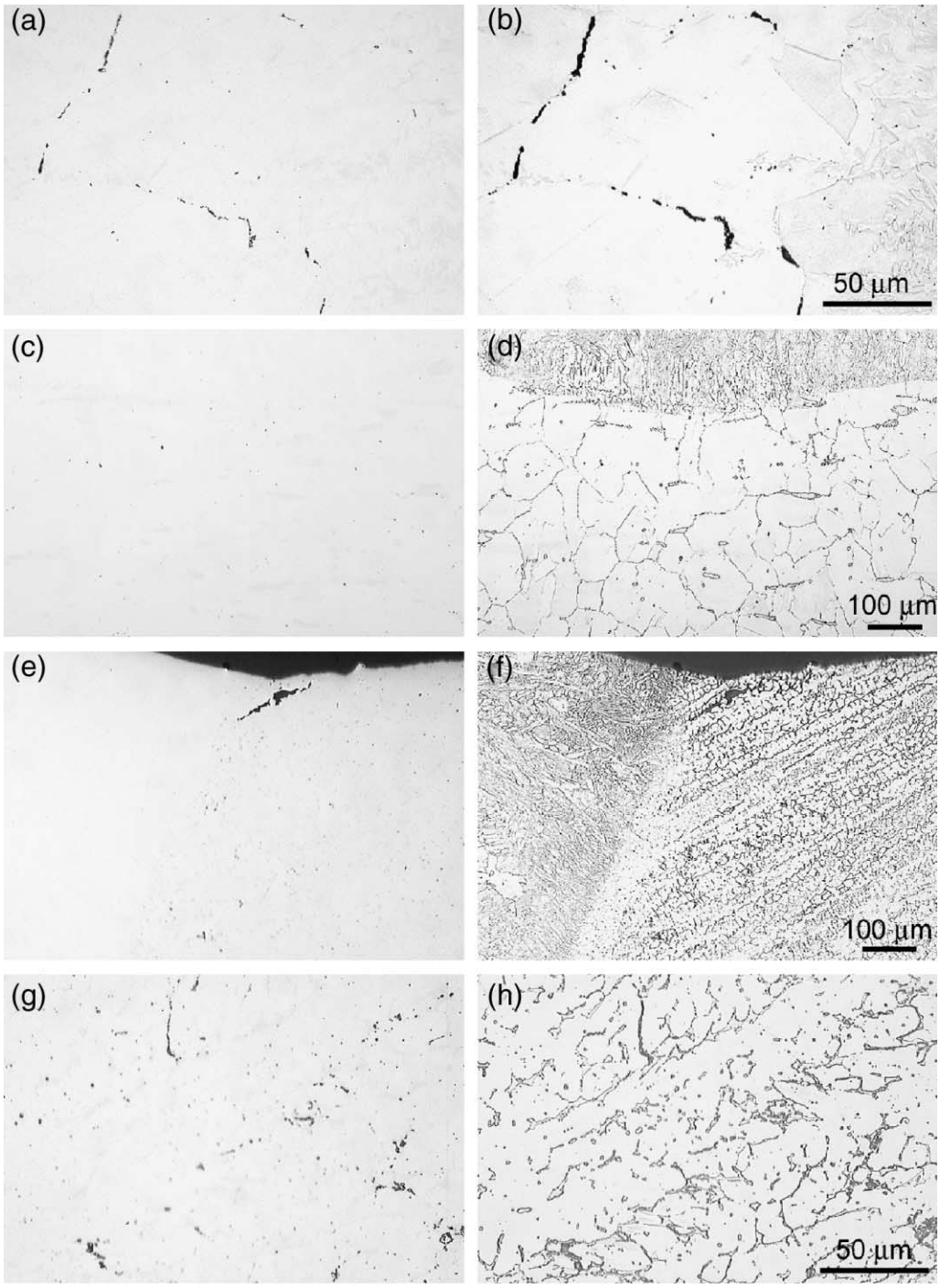

Fig. 3. Typical cross-sectional micrographs of the 1 MJ/m build-up welded specimen. Micrographs (a), (c), (e) and (g) are related to an unetched specimen, (b), (d), (f) and (h) are related to an etched status. The observed areas are indicated in Fig. 2.

experienced at the neck point. The helium bubbles continue to grow until the last pass, and the diameter becomes approximately twice one calculated at the bottom point. In the SAW weld metal, the helium

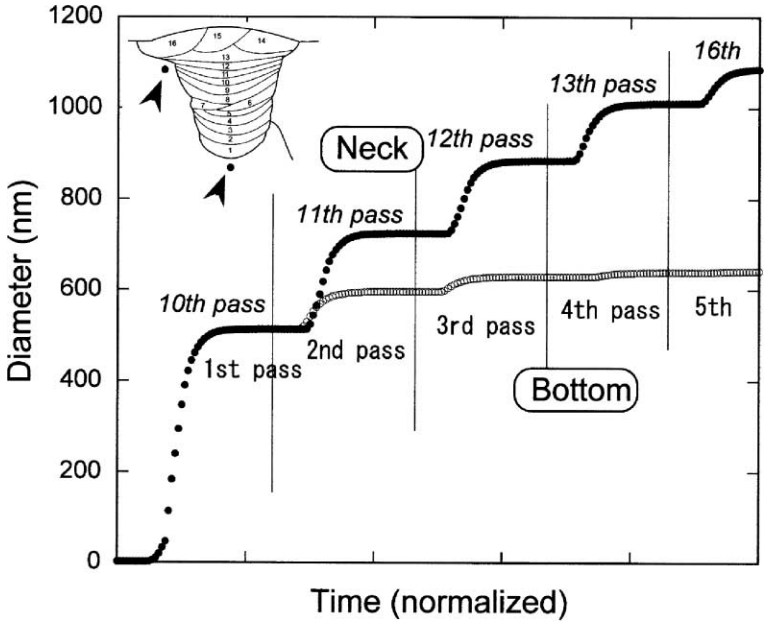

Fig. 4. Calculated changes in helium bubble diameter at the neck and bottom points of a groove (0.2 mm from the fusion line) for the 1 MJ/m build-up welded specimen containing 0.5 appm helium. The horizontal axis is normalized by time of each thermal cycle.

concentration is more than three times greater than that in the base metal, and the bubble diameter is calculated to be about 1.33 μm, whereas the corresponding value in the base metal is 1.08 μm.

5. Summary

Weldability of neutron-irradiated Type 304 SS containing 0.5 appm helium has been studied by multi-pass TIG welding at heat inputs of 0.2, 0.4 and 1 MJ/m. Main results are summarized as follows.

1. Neither visible cracks nor traces of helium bubbles were found in the one- to three-pass bead-on-plate welding tests for all weld heat inputs.
2. Cracks or bubbles were not observed in the 0.4 MJ/m build-up welding of a groove. However, when the process was performed at a heat input of 1 MJ/m, helium bubbles were found on grain boundaries in the area within 0.6 mm from the fusion line in the base metal, and surface cracking and bubbles were observed on dendrite boundaries on the side of the SAW weld metal containing 1.8 appm helium.
3. Helium bubbles were concentrated in the neck part of the groove, they were not found around the bottom part. From the results of a helium bubble growth calculation, this behavior seems due to the difference in thermal cycles between the upper and lower zone of the groove.

References

[1] W.R. Kanne Jr., Welding J. 67 (1988) 33.
[2] C.A. Wang, M.L. Grossbeck, B.A. Chin, J. Nucl. Mater. 225 (1995) 59.
[3] H.T. Lin, M.L. Grossbeck, B.A. Chin, Metall. Trans. A 21A (1990) 2585.
[4] W.R. Kanne Jr., G.T. Chandler, D.Z. Nelson, E.A. Franko-Ferreira, J. Nucl. Mater. 225 (1995) 69.
[5] K. Watanabe, S. Jitsukawa, S. Hamada, T. Kodaira, A. Hishinuma, Fus. Eng. Des. 1 (1996) 9.
[6] S.H. Goods, N.Y.C. Yang, Metall. Trans. A 23A (1992) 1021.
[7] K. Asano, S. Nishimura, Y. Saito, H. Sakamoto, Y. Yamada, T. Kato, T. Hashimoto, J. Nucl. Mater. 264 (1999) 1.
[8] S. Nishimura, R. Katsura, Y. Saito, W. Kono, H. Takahashi, M. Koshiishi, T. Kato, K. Asano, J. Nucl. Mater. 258–263 (1998) 2002.
[9] E.V. van Osch, D.S. d'Hulst, J.G. van der Laan, Fus. Technol. 95 (1995) 399.
[10] K. Nakata, S. Kasahara, H. Takeda, M. Oishi, in: F.P. Ford, S.M. Bruemmer, G.S. Was (Eds.), Proceedings of the Ninth International Symposium on Environmental Degradation of Materials in Nuclear Power Systems–Water Reactors, TMS, 1999, p. 767.

[11] C.H. Zhang, K.Q. Chen, T.S. Wang, J.G. Sun, D.Y. Shen, J. Nucl. Mater. 245 (1997) 210.
[12] T. Hashimoto, M. Mochizuki, in: M.L. Hamilton, A.S. Kumar, S.T. Rosinski, M.L. Grossbeck (Eds.), ASTM STP 1366, ASTM, PA, 2000, p. 973.
[13] T. Hashimoto, N. Yanagida, K. Koshiishi, S. Kawano, H. Sakamoto, K. Nakata, M. Oishi, Numerical analysis on the weldability of neutron-irradiated stainless steels, Proceedings of the 6th International Seminar on Numerical Analysis of Weldability, October 2001, Graze, Austria.
[14] D. Hull, D.E. Rimmer, Philos. Mag. 4 (1959) 673.
[15] T. Saito, M. Shiwa, A. Yamada, S. Nakahigashi, K. Nakata, M. Oishi, 82nd Anneal American Welding Society Convention Abstract, Cleveland, OH, 2001, p. 97.